

AUTOMATIC NEUROPHYSIOLOGICAL IDENTIFICATION OF THE HUMAN STN BASED ON UNSUPERVISED METHODS

K.M.L. Menne*, S. Kondra* and U.G. Hofmann*

* Institute for Signal Processing, University of Lübeck, Lübeck, Germany

hofmann@isip.uni-luebeck.de

Abstract: The human subthalamic nucleus (STN) is one of the main target regions for the implantation of deep brain stimulation electrodes for the treatment of Parkinson's disease. Next to standard stereotactic methods, intraoperative microelectrode recordings help to identify this target region with a high degree of accuracy. However, a reliable and automatic online analysis of the intraoperatively recorded signals is hard to achieve. First attempts to automatically characterize STN-activity employ features calculated for so called spiketrains that get extracted from the raw recorded data by methods of spike detection and spike sorting. The results of this approach can severely depend on the user's experience and methodological preferences, and thus are subject to human error and inconsistency. We show in this contribution that alternatively a reliable, automatic classification of STN activity is very well feasible by employing statistical signal processing methods and unsupervised classification. The methods were tested on real microelectrode data recorded in the human STN. They got integrated into a novel 32-channel data acquisition system for intraoperative recordings, for which reliable, automatic classification methods are indispensable.

Introduction

Deep brain stimulation (DBS) has gained great importance in the treatment of movement disorders like Parkinson's disease. In order to elicit the desired therapeutic effect, the stimulation electrodes need to be implanted very accurately in the interesting target region during a functional stereotactic neurosurgery. The target region in the case of Parkinson's disease is one of Nucleus subthalamicus (STN), globus pallidus pars interna (GPI) or ventralis intermedius nucleus (VIM). In Europe, the deep brain structure STN is chosen most frequently because of the good therapeutic effects that are achievable. Preoperatively, neurosurgeons try to identify the target region on the patient's computertomography (CT) and/or magnetic resonance (MRT) images and plan a straight trajectory from the skull towards this region. However, because of the small size of the deep brain structures and the rather poor resolution of the imaging material, the target region can hardly be identified. Besides, localization based on image data gets corrupted intraoperatively because of physiologic effects like brainshift caused by the loss of intracerebral fluid. Because of these

drawbacks microelectrode recordings are performed intraoperatively to verify the target region. Since each brain region is assumed to generate a distinct, neural activity pattern, a neurophysiological identification of the target region is possible.

However, a reliable, automatic classification of the recorded signals and thus an automatic neurophysiological identification of the target region was not possible so far. Most data acquisition systems currently in use do not offer methods to solve this task. Instead, experienced neurosurgeons and neurophysiologists have to characterize the signals manually - a severe problem for less experienced teams.

First attempts for automatic data analysis employ features calculated on spiketrains [1,2]. Spiketrains represent in a binary fashion the spiking activity of a single neuron over time. Methods of spike detection and spike sorting need to be applied in order to extract the spiketrains from the raw recorded data. Many approaches of spike detection and spike sorting require a high degree of user interaction and thus the results can again severely depend on the user's experience, and accordingly are subject to human error and inconsistency. Consequently, features like e.g. the firing rate of a neuron calculated for spiketrains from one and the same brain region by different groups can vary in a wide range and complicate an automatic classification [3,4,5,6]. Therefore there is a need for alternative methods that require a low degree of user interaction but provide for reliable signal features that can be used for an automatic classification of brain activity.

Another reason that motivates the quest for automatic methods like this is the advent of data acquisition systems that are capable of processing a high number of channels simultaneously. In the framework of a project funded by the German Ministry of Education and Research a novel data acquisition system was developed that supports intraoperative recordings with a new 32-channel probe [7,8,9,10]. Data acquisition systems currently available only support up to 5 channels. Concerning these systems there is no urgent need to replace a manual inspection or a semi-automatic classification of data requiring a high degree of user interaction. Experienced neurosurgeons and neurophysiologists are able to characterize this number of channels. But obviously the same cannot be true for 32 channels.

Materials and Methods

Data acquisition: The presented methods were tested on data originating from recordings performed during stereotactic implantations of electrodes for deep brain stimulation in the subthalamic nucleus of six patients suffering from Parkinson's disease at the University-Hospital Hamburg-Eppendorf. All patients gave free and informed consent concerning the intraoperative microelectrode recordings. Spontaneous neural activity was recorded using conventional tungsten single-electrodes (microtargeting electrode 291A; FHC, Bowdoinham, USA; impedance 0,5-1,5 MΩ) on up to 4 parallel trajectories. A 4 channel microelectrode recording unit (Leadpoint®; Medtronic, Inc., Minneapolis, USA) was employed for visualization and permanent storage of the data. Signals were bandpass-filtered between 500 and 5000 Hz and were digitized at a sampling rate of 24 kHz. Recording sequences lasted typically between 0,5 and 5 minutes. Signals alongside the trajectories were classified by an experienced neurophysiologist into one of two classes: STN-signal or non-STN-signal originating from a neighbouring brain region.

Data analysis: Data were analyzed post surgery with the help of the Matlab software package (Mathworks, Inc., Natick, USA). Instead of extracting spiketrains from the data and analyzing them, we calculated different statistical measures for the raw signals [11]. The following list gives names and alternative names of the features and the abbreviations that are used throughout the text and figures.

- first moment (arithmetic mean, Sigm)
- second moment (power, Sigm2)
- third central moment (skewness, Sigz3)
- fourth central moment (kurtosis, Sigz4)
- maximum amplitude (Sigmax)
- minimum amplitude (Sigmin)
- median amplitude (Sigmed)
- root mean square (RMS)
- entropy (Ent)
- frequency at peak in power spectral density estimate (maxF)
- P250-2500 (PSD)

This initial set of commonly used features in statistical signal processing was computed for signal stretches of 30 second duration. The first and second moment were calculated according to

$$m_p = \frac{1}{N} \sum_{n=0}^{N-1} x(n)^p$$

where N denotes the number of samplepoints of signal stretch $x(n)$ and p equals 1 or 2, respectively. Central moments were computed as

$$z_p = \frac{1}{N} \sum_{n=0}^{N-1} (x(n) - m_1)^p$$

where p equals 3 or 4 respectively, and m_1 denotes the first moment. The central moments were normalized by the square root of the p -th power of the variance z_2 . The median amplitude was computed for the absolute amplitude values. Entropy was calculated based on the amplitude histogram according to the equation

$$H = - \sum_{i=1}^m h_i \text{ld } h_i$$

Here, h_i denote the relative occurrences of the quantized amplitudes. In this case m equals 4096 because of the 12 bit digitization. ld denotes the logarithm to the basis 2.

The last two features mentioned were calculated on the basis of an estimate of the power spectral density of the signals. For estimating the power spectral density, we employed the Welch method. Signal stretches of 4.76 seconds got divided into 7 windows of 0.68 seconds in length, overlapping by 50 percent. The employed window was the Hamming window. The value that is referred to here as PSD was introduced by Pesenti et al. [12] in a similar fashion. For this value, the values in the frequency band from 250 Hz to 2500 Hz get summed up.

Among this initial set of features those features were to be selected, that are discriminative with respect to the task of distinguishing signals recorded in the STN from signals recorded in neighbouring brain regions. Because the recorded signals are random signals, the calculated signal features are random numbers as well. The question at hand was to decide, which features show a different distribution when calculated for STN-signals compared to when calculated for non-STN-signals. For this purpose Wilcoxon rank sum tests were conducted. We chose this non-parametric test because of the small size of the random samples. When the microelectrode is introduced into the brain along one trajectory, recordings at about 20 different positions are performed. Some of the recording positions are within STN, others in neighbouring brain regions. Based on the manual classification by the experienced neurophysiologist we knew which signals were recorded in STN or an alternative brain region and could build random samples for features calculated for STN-signals or non-STN-signals accordingly - sometimes comprising only a few values. We conducted 12 Wilcoxon rank sum tests for data calculated on 12 trajectories that definitely passed the STN.

Unsupervised classification: Features found to be discriminative were used as input for unsupervised classification with the k-means classifier. Two classes were to distinguish: STN-activity and neural activity of adjacent brain structures. We used random initialization to define initial cluster centers.

Results

The results of the Wilcoxon rank sum tests for the 12 investigated trajectories are summarized in Figures 1

and 2. The trajectories are numbered from 1 to 12 on the abscissas. The investigated features are denoted on the ordinates. The connecting lines are intended to support readability. In the subfigures of Figure 1, a H-value of 1 indicates that the respective feature denoted at the ordinate has a significantly different distribution when calculated for STN-signals on the respective trajectory compared to when calculated for non-STN-signals on this trajectory. The P-values in Figure 2 indicate how reliable the obtained results are - the lower the P-value, the lower the probability of error.

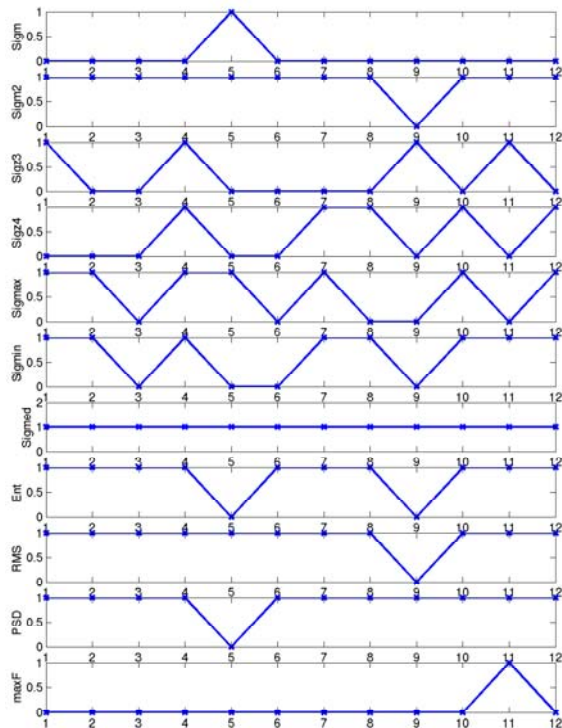


Figure 1: Results of Wilcoxon rank sum test (H-value) for 12 trajectories. For details see text.

The presented results indicate, that the power, the median amplitude, the entropy, the rms value and the PSD value show a significantly different distribution when calculated for STN-signals compared to when calculated for non-STN signals on the majority of trajectories. Features like the arithmetic mean, statistical moments of higher order, the maximum or the minimum amplitude do not show a significantly different distribution for STN-signals. They can hardly be used to identify STN-activity.

The histograms in Figure 3 indicate the distributions of the five features that were found to be most discriminative. For these histograms we generated two samples, one comprising the respective feature calculated for STN-signals on one of the 12 trajectories, the other one comprising the respective feature calculated for non-STN-signals. Obviously the features take higher values when calculated for STN-signals. This observation is explicable with an increased level of neuronal background noise in the STN compared to

other brain regions and high spiking activity of STN neurons.

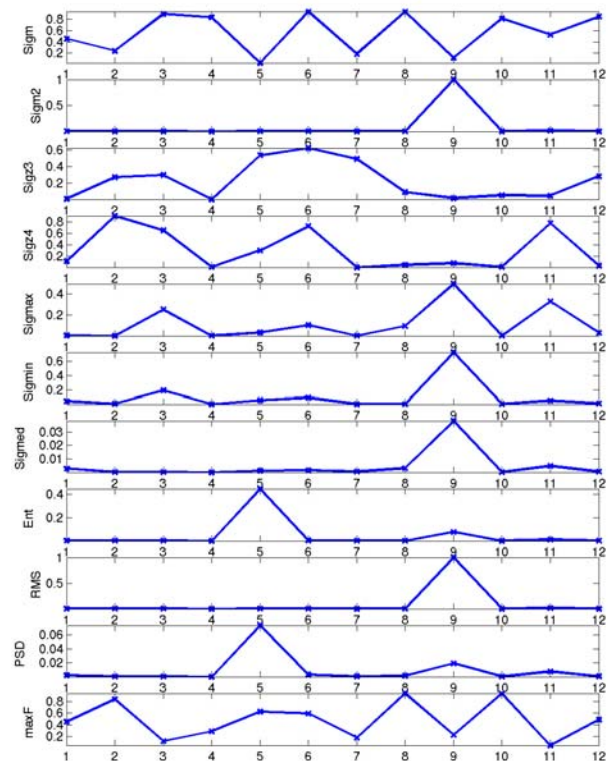


Figure 2: Results of Wilcoxon rank sum test (P-value) for 12 trajectories.

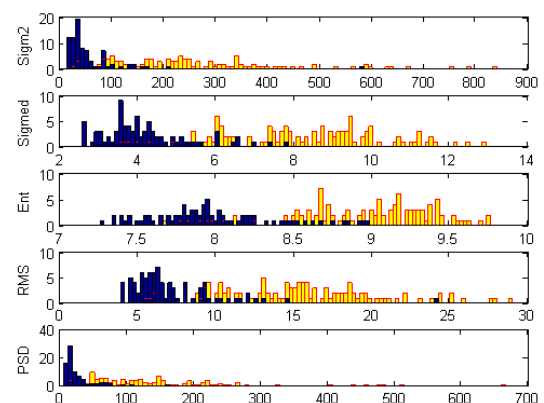


Figure 3: Distribution of feature values calculated for STN-signals (yellow) and signals originating from neighbouring brain regions (blue). The value ranges are denoted on the abscissas, the relative occurrences on the ordinates. Each time 100 bins were used.

The discriminative features Sigm2, Sigmmed, Ent, RMS and PSD were used as input for the unsupervised k-means classification. Figures 4 and 5 show the results of a one-dimensional automatic classification when only the entropy or the median amplitude, respectively, is taken as input and compare it against the manual classification by the experienced neurophysiologist. The

results were obtained for data recorded on one trajectory from one patient - the same one in both figures. On the ordinates, the individual recording positions along the trajectory are denoted in μm . Negative numbers indicate positions above the planned target point at $0 \mu\text{m}$, positive numbers indicate positions below the planned target point. The black horizontal lines indicate the result of the manual classification. Signals recorded at positions between $-6000 \mu\text{m}$ and $-500 \mu\text{m}$ were characterized as STN-activity by the neurophysiologist. The color of the stars indicates the result of the automatic classification, where the color itself does not have a meaning.

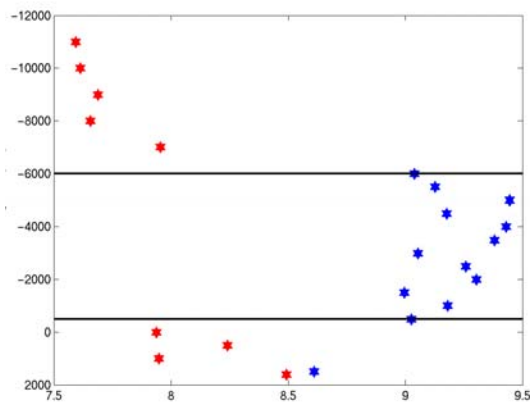


Figure 4: Comparison of automatic and manual classification results. For automatic classification the entropy feature was used. The entropy values at the respective recording positions are given in bit on the abscissa. Ordinate gives a measure for the depth of recording position. Distance between lines was found by a neurophysiologist to represent STN (see text).

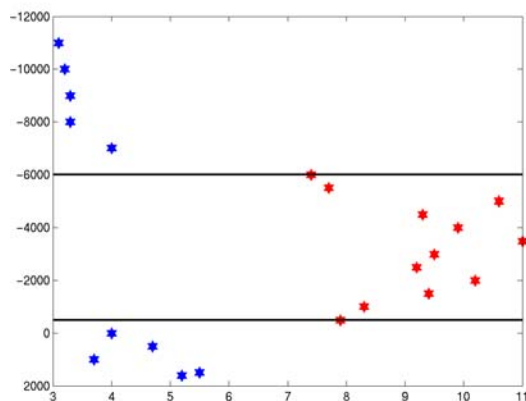


Figure 5: Comparison of automatic and manual classification results. For automatic classification the median amplitude feature was used. The median amplitude values at the respective recording positions are given in μV on the abscissa.

In both figures, manual and automatic classification results show a high degree of agreement. When regarding entropy (Figure 4), only one misclassification

is observed at $1800 \mu\text{m}$ below the planned target point. When regarding the median value (Figure 5), there is an exact agreement between automatic and manual classification.

The results presented in Figures 4 and 5 were obtained on one of four parallel trajectories from the same hemisphere of one patient. Automatic classification results obtained on all four parallel trajectories for the median value are shown in Figure 6. The trajectory regarded in Figures 4 and 5 corresponds to the lateral trajectory at xy-coordinates $(-2,0)$. On this trajectory, the two red plains indicate the corresponding manually and automatically determined borders of the STN. For the anterior $(0,-2)$ and central $(0,0)$ trajectory, automatic and manual classification results differ by only one position (equal to $500 \mu\text{m}$), indicated by the blue and red plains. The lateral trajectory $(0,2)$ does not pass the STN, and indeed there is no STN-activity automatically classified.

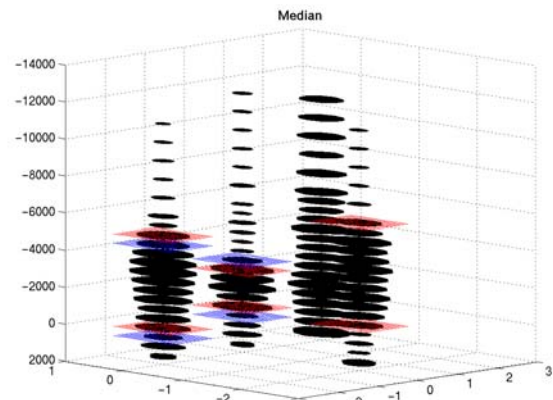


Figure 6: Comparison of automatic and manual classification on 4 parallel trajectories. The recording position is indicated on the z-axis. The size of the ellipses indicates the value of the median calculated for the signal recorded at the respective position. Red plains indicate the automatic classification result, blue plains the manual classification result.

Our test data contained 12 trajectories that were passing the STN. The classification results for these 12 trajectories are summarized in Table 1. Results are given for power, median amplitude, rms value and entropy. Sensitivity indicates the percentage of correctly classified STN-activity of all STN-activity on the 12 trajectories. That means

$$\text{sensitivity} = \text{TP} / (\text{TP} + \text{FN})$$

where TP denotes the number of STN-signals that were classified as STN-signals and FN denotes the number of STN-signals that were classified as non-STN-signals. Given the classification by the experienced neurophysiologist, e.g. 95% of STN-signals were also correctly classified automatically when regarding the entropy feature. However, since there are also sum false positive classifications, the percentage of

correctly identified STN-borders ranges below the sensitivity values. The results show that entropy is the most suitable feature for automatic characterization of STN-activity.

Table 1: Results of automatic classification of STN-activity on 12 trajectories when using different features. "Correct borders" means that STN-entry and STN-exit of the microelectrode were correctly determined automatically.

Statistical measure	Sensitivity	Correct borders
Sigm2	52%	32%
Sigmed	70%	53%
RMS	71%	58%
Ent	95%	68%

Discussion

The presented results show that an automatic characterization of human STN-activity is feasible with easy means. In order to extract discriminative features as input for classification routines it is not necessary to conduct error-prone spike detection and spike sorting and calculate features of spike trains. Instead, statistical measures calculated for the raw signals allow for a reliable automatic classification. The request for a low degree of user interaction is fulfilled as well. The statistical measures can be calculated without almost any user interaction. The user has only to decide once, how long the signal stretches should be on which to calculate the features. We made good experiences with signal stretches of 30 seconds in length. Parameters for how to estimate the power spectral density also have to be determined only once in the beginning. Presented results were obtained offline, but are in principle accessible for online analysis as well.

All presented features are scalar values. This allows on the one hand for a clearly arranged visualization and on the other hand for easy comparisons. Calculated features can be stored in a database and can be compared against intraoperatively calculated features.

The interesting question arises, whether the same features are suitable for characterizing activity of the alternative target regions GPi or VIM. Since we did not have manually classified signals from these regions at hand, this is work in progress.

Conclusions

The presented methods got incorporated into a new data acquisition system for 32 channels [7,8,9]. This navEgate data acquisition system allows for the simultaneous recording of 32 channels with a novel probe comprising 32 recording sites on one shaft system [10] (commercially available at ThomasRecording GmbH, Giessen, Germany). This way, a depth profile of neuronal activity becomes available at one glance.

While preclinical studies of the system are on the way, we are convinced that the possibility to record neural depth profiles combined with our fast and reliable automatic data analysis methods will speed up intraoperative microelectrode recordings considerably, while providing direct benefit to the patient. To additionally assist less experienced teams, an electrophysiological database, the navEbase database [13], is integrated into the data acquisition software of the novel system. This database offers the possibility mentioned above to compare intraoperatively currently computed features against those stored in the database originating from different brain regions. This feedback from navEbase will assist teams in questionable cases.

Acknowledgements

We thank Christian K.E. Moll and Prof. Dr. A. Engel, University Hospital Hamburg-Eppendorf, for the kind provision of data and the manual analysis of the signals.

References

- [1] FAVRE, J. and BAUMANN, T. (2004): 'Signal Processing and Pattern Recognition in Microelectrode Recordings', in ISRAEL, Z. and BURCHIEL, K. J. (Eds): 'Microelectrode Recording in Movement Disorder Surgery', (Thieme, New York), pp. 100-110
- [2] MCNAMES, J. (2004): 'Microelectrode Signal Analysis Techniques for Improved Localization', in ISRAEL, Z. and BURCHIEL, K. J. (Eds): 'Microelectrode Recording in Movement Disorder Surgery', (Thieme, New York), pp. 119-129
- [3] HUTCHISON, W. D., ALLAN, R. J. et al. (1998): 'Neurophysiological Identification of the Subthalamic Nucleus in Surgery for Parkinson's Disease', *Ann Neurol.*, **44**, pp. 622-628
- [4] LEVY, R., HUTCHISON, W.D., LOZANO, A.M., and DOSTROVSKY, J.O. (2000): 'High-frequency Synchronization of Neuronal activity in the subthalamic nucleus of Parkinsonian Patients with Limb Tremor', *J Neurosci*, **20**, pp. 7766-7775
- [5] MAGARIÑOS-ASCONE, C.M., FIGUEIRAS-MENDEZ, R., RIVA-MEANA, C., and CORDOBA-FERNANDEZ, A. (2000): 'Subthalamic Neuron Activity Related to Tremor and Movement in Parkinson's disease', *Eur J Neurosci*, **12**, pp. 2597-2607
- [6] RODRIGUEZ-OROZ, M. C., RODRIGUEZ, M. et al. (2001): 'The Subthalamic Nucleus in Parkinson's Disease: Somatotopic Organization and Physiological Characteristics', *Brain*, **124**, pp. 1777-1790
- [7] MENNE, K.M.L., FOLKERS, A., SCHUHART, H. and HOFMANN, U.G. (2003): 'Neurosurgery by Multichannel Electrophysiology, 3DNavigation, and Customized Database', *Biomedizinische Technik*, **48 - Ergänzungsband 1**, pp. 500-501
- [8] MENNE, K.M.L., BAER, M., DETEMPLE, P. and HOFMANN, U.G. (2004): 'A novel system for

- stereotactic functional neurosurgeries', *Biomedizinische Technik*, **49 - Ergänzungsband 2**, pp. 770-771
- [9] MENNE, K.M.L., MOLL, C.K.E. et al. (2004): 'On-line 32 Channel Signal Processing and Integrated Database Improve Navigation during Cranial Stereotactic Surgeries', Proc. of CARS 2004, Chicago, USA, 2004, *International Congress Series*, **1268**, pp. 443-448
- [10] HOFMANN, U.G., BÄR, M., DETEMPLE, P., KINDLUNDH, M., NORLIN, P. (2004): 'Acute Multisite Recording Probes for Neurons in Mice and Men', *mstnews*, **1/2004**, pp.14-16
- [11] MENNE, K.M.L. (2005): 'Computerassistentz zur Implantation von Tiefenhirnstimulatoren - Von der Merkmalsbestimmung für Gehirnsignale zur Datenbank für Elektrophysiologie', PhD Thesis, to be published
- [12] PESENTI, A., ROHR, M. et al. (2003): 'The Subthalamic Nucleus in Parkinson's Disease: Power Spectral Density Analysis of Neural Intraoperative Signals', *Neurol Sci*, **24**, pp. 367-374
- [13] MENNE, K., HOFMANN, U. (2004): 'Neurowissenschaftliche Datenbanken - eine Herausforderung', *Datenbank-Spektrum*, **10**, pp. 5-13